# ULTIMATE LOAD CAPACITY FOR SPATIALLY LOADED BEAMS OF THIN WALLED OPEN CROSS-SECTIONS CONSIDERING ALL SHEAR EFFECTS

**Mohamed Abdel Fattah Diwan**
Structural Engineering Department, Faculty of Engineering,
Alexandria University, Alexandria, Egypt.

ABSTRACT

The present paper develops the ultimate load capacity for spatially loaded beams composed of thin walled open cross-sections where all shear effects, stresses, deflections as well as resistances, are included in the analysis. The general description of the constitutive behavior for isotropic materials is reduced for the extended one-dimensional beam case to a finite constitutive law. All non-linear effects, deflections and material non-linearities, are considered iteratively. By the use of the derivated comprehensive calculation program essential differences to a shear- neglecting calculation are demonstrated by several examples.

SUMMARY

The importance of incorporating all variables in the analysis of beams ultimate loads is currently maximized. Most newly developed codes include the ultimate design method.Most works dealing with the shear deformations were either for structures subjected to shearing forces or elastically loaded. The influence of shearing force is investigated by Windels [1] for inelastic plane systems, where interaction relations are given for sections under a combined action of normal force, shearing force and bending moment. The effect of shear on fork supported one span beams, spatially loaded in the elasto-plastic range is investigated by Bamm [2] . Bamm kept the shear stress distribution of the elastic loading constant through the plastic range. A maximum difference in the ultimate load capacity was found equals to 3.7% comparing to the case where the shear effects were neglected. This value was only true for his case study, where redistribution of the shearing force and the shear stress was not allowed. Maier [3] introduced the first work involving all effects of shear on spatially loaded structures. A beam-model including shear effect was considered as a basis for the geometrical detection, and the von Mises yield criteria for the equivalent yield area was used during the plastic range.

The present work develops the solution of spatially loaded beams composed of thin walled open cross-sections considering all shear effects, stresses and material resistances, within the elasto-plastic loading conditions.

The second-order theory for spatially loaded beams with shear deformation developed in [4] is modified and used to determine the ultimate load capacity for beams having thin walled open cross-sections. Hereby the von Mises yield criteria is employed to develop a finite constitutive law represents the behavior of the isotropic material for the extended beam case in the elasto-plastic range where normal, and shear stresses are applied. For each loading step the nonlinearity of the equilibrium equations and material resistances is considered iteratively. And by increasing the loadings in increments the ultimate load capacity will be obtained.

Several demonstrated examples are given to illustrate the accuracy and the efficiency of the developed method and the computer program. Examples are intended to clearly show the influence of including shear effects on the ultimate load capacity of beams. Comparisons showed the difference related to the exact solution, done here, and the approximate ones.

## MATERIAL RELATIONS PRINCIPALS

The true global triaxial stress tensor $\sigma_{ij}$ can be translated to a fictitious equivalent uniaxial stress $\sigma_e$ by replacing the yield stress $\sigma_y$ by the equivalent stress $\sigma_e$ in the von Mises yield condition, which gives

$$\sigma_e^2 = 3 I_2' \qquad (1)$$

where $I_2'$ represents the second invariant of the stress deviator $\sigma_{ij}'$, and defined by,

$$I_2' = \frac{1}{2}\sigma_{ij}'\sigma_{ij}' \quad (2)$$

Equation 1 is valid not only for linear elastic range, but also for elastic-plastic deformations. A complete proof to Eq.1 and Eq.2 is given in [5] .

The relationships between stresses and strains in the deformation increments theory are given by the Prandtl-Reuss equations

$$d\epsilon_{ij}' = \frac{d\sigma_{ij}'}{2G} + \sigma_{ij}' \cdot \frac{3}{2}\frac{d\epsilon_e^p}{\sigma_e} \quad (3)$$

where $\varepsilon_{ij}'$ represent the strain deviator, G is the elastic shear modulues and

$\epsilon_e^p$ is the plastic equivalent strain.

Integrating Prandtl-Reuss equations, Eqs 3, yields finite deformation theory [5]. For small elastic-plastic deformations (elastic and plastic deformations have the same order) a very good approximate solution could be obtained, despite its quick convergence which proves its simplicity and straightforwardness. The total strains are given by

$$S.\varepsilon_{ij} = (1+\nu_{ep})\sigma_{ij} - \nu_{ep}\sigma_{kk}\delta_{ij} \quad (4)$$

S is the secant modulues, and $\upsilon_{ep}$ is the elastic plastic Poisson's ratio

$$S = \frac{\sigma_e}{\varepsilon_e} \quad (5)$$

$$2\nu_{ep} = 1 - (1-2\nu)\frac{S}{E} \quad (6)$$

$\upsilon$ and E are the Poisson's ratio, and the modulues of elasticity respectively.

## REDUCTION OF THE MATERIAL EQUATIONS TO THE CONSIDERED BEAM STRESSES

Considering shear stress in beams, the only existing terms other than zeros in the stress tensor $\sigma_{ij}$ are $\sigma_{11} = \sigma_x$ longitudinal normal stress

$\sigma_{12} = \sigma_{21} = \tau_{xs}$ cross-sectional shear stress

Also the only existing terms, other than zeros in the strain tensor $\in_{ij}$ are

$\varepsilon_{11} = \varepsilon_x$ longitudinal normal strain

$$\varepsilon_{22} = \varepsilon_{33} = -\nu_{ep}\cdot\varepsilon_x$$

$\varepsilon_{12} = \varepsilon_{21} = \gamma_{xs}$ / 2 shear strain / 2

Using i = j = 1 in Eq.4 gives

$$\sigma_x = S.\ \varepsilon_x \quad (7)$$

And for i = 1 , and j = 2 the relationship between shear stress $\tau_{xs}$ and shear strain $\gamma_{xs}$ is

$$\tau_{xs} = G_{ep}\cdot\gamma_{xs} \quad (8)$$

where the elastic plastic shear modulues $G_{ep}$ is given as

$$G_{ep} = \frac{S}{2(1+\nu_{ep})} \quad (9)$$

The equivalent uniaxial stress $\sigma_e$ representing the von Mises yield criteria for the beam case is obtained from Eq.4 by applying the beam stress tensor, i.e.

$$\sigma_e = \sqrt{\sigma_x^2 + 3\tau_{xs}^2} \quad (10)$$

The equivalent longitudinal strain $\varepsilon_e$ can be derived by substituting equations 7 and 8 in Eq.10 and using equations 5 and 9, hence

$$\varepsilon_e = \sqrt{\varepsilon_x^2 + 3\gamma_{xs}^2\left(\frac{1}{2(1+\nu_{ep})}\right)^2} \quad (11)$$

## STRAIN-DISPLACEMENT RELATIONSHIPS

According to the coordinate systems and displacement directions shown in Figure (1) and by following the analysis developed in [4] , a refined displacement field is determined by employing the method of successive approximations.

The strain-displacement relationship associated with the modified displacement field are derived and modified to be applied in the elastic-plastic range. For the longitudinal strain

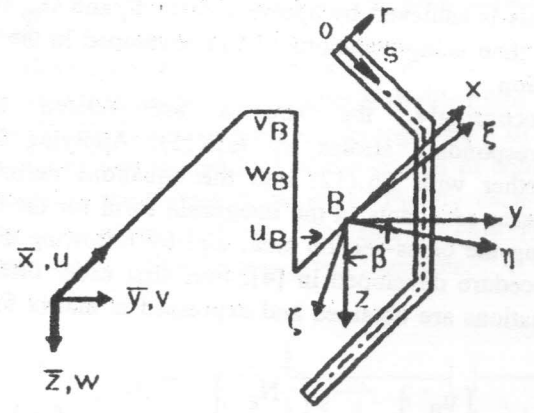


**Figure 1.** Typical cross-section and coordinate systems

$$\varepsilon = u_B' - y v_B'' - z w_B'' - \omega \beta'' - y(w_B'' \beta) + z(v_B'' \beta) + (y^2 + z^2)\left(\frac{1}{2}\beta'^2\right)$$

$$+ \frac{1}{2}(v_B'^2 + w_B'^2) + \Gamma_y . \psi' + \Gamma_z . \phi' + \Gamma_\omega . \Omega' \qquad (12.a)$$

The shear strain satisfying the force equilibrium in the longitudinal direction is expressed by

$$\gamma = 2\, r\, \beta' + \frac{1}{G_i t}[S_y . \psi + S_z . \phi + S_\omega . \Omega] \qquad (12.b)$$

In the above equations $\psi$ , $\phi$ and $\Omega$ denote the third derivatives of the displacements $v_B$ , $w_B$ and $\beta$ which are to be evaluated using initial displacement values obtained by neglecting the shear effect.

The following extended cross-section properties are introduced to simplify the expressions

$$S_y = \int_o^s S_i . y\, dF, S_z = \int_o^s S_i . z . dF \text{ and } S_\omega = \int_o^s S_i . \omega . dF \quad (13.a\text{-}c)$$

together with

$$\Gamma_y = \int_o^s \frac{S_y}{G_i t} . ds - \int_o^{s_B} \frac{S_y}{G_i t} ds$$

$$\Gamma_z = \int_o^s \frac{S_z}{G_i t} . ds - \int_o^{s_B} \frac{S_z}{G_i t} ds$$

$$\Gamma_\omega = \int_o^s \frac{S_\omega}{G_i t} . ds - \int_o^{s_B} \frac{S_\omega}{G_i t} ds \qquad (14.a\text{-}c)$$

where $S_i$ and $G_i$ indicate the secant modulues, and the shear modulues associated with each element having cross section area equals to dF.

## EQUILIBRIUM EQUATIONS AND BOUNDARY CONDITIONS

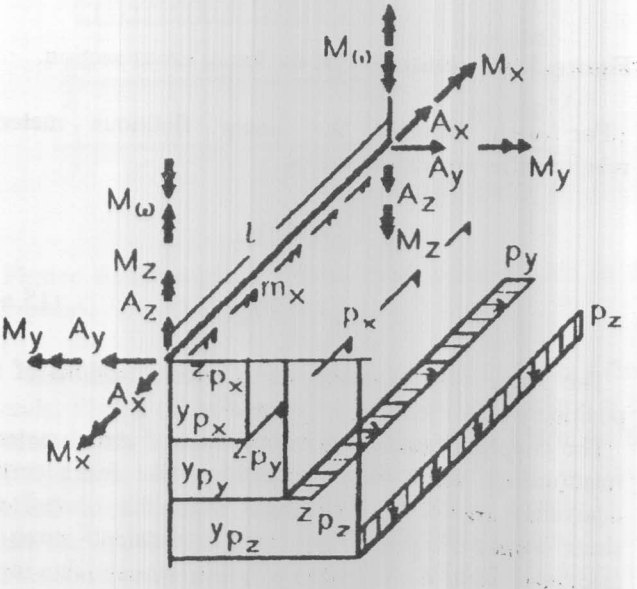


**Figure 2.** Uniformly distributed loads and the rand stress resultants.

Consider the straight member Figure (2) under the action of the distributed external forces acting along the beam part length l and externally applied stresses at both ends. Applying the virtual work principle, a system of differential equations of the first order is derived [4] .

## STRESS RESULTANT-DISPLACEMENT RELATIONSHIPS

Referring to the finite material law given in the second section, the material nonlinearity is introduced in the analysis by discretizing the beam cross-section into a fine mesh, Figure (3).

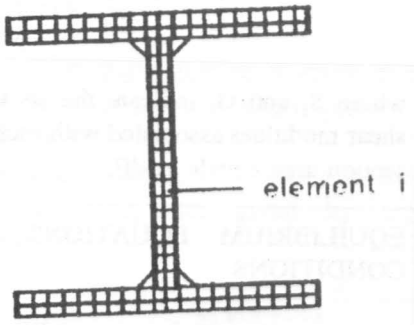


**Figure 3.** Discretization of the beam cross-section.

For each element the linear fictitious material relationships are expressed as

$$\sigma_\xi = S_i \cdot \epsilon_\xi$$

$$\tau_{\xi s} = G_i \cdot \gamma_{\xi s} \qquad (15.a\text{-}b)$$

The linear coefficients $S_i$ and $G_i$ are functions of the position of the element $x_i$ , $y_i$ and $z_i$

The coupling between the fictitious and actual material relationships exists in the condition that for a certain equivalent strain $\in_e$ calculated from the normal and shear strains $\in_\xi$ and $\gamma_{\xi s}$ ,the equivalent stress $\sigma_e$ calculated from the normal and shear stresses due to the fictitious relationships given in Eq.(15) must yield the same value generated using the actual relationship, Figure (4).

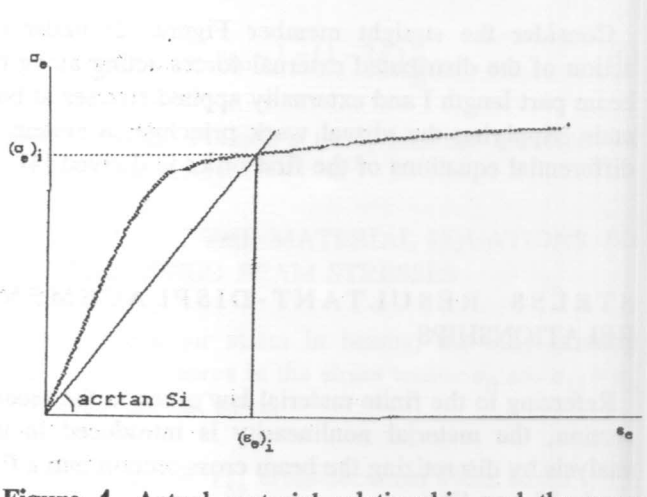


**Figure 4.** Actual material relationship and the secant modulues S.

This is achieved by applying S for $S_i$ and $G_{ep}$ for $G_i$ and then using equations (7-11) developed in the second section.

Accordingly, the stresses are related to the corresponding strains by Eq.(15). Applying Eq.(15) together with Eq.(12) into the equations defining the stresses resultants in the integrable form for the stresses along the cross-section area, and by following the same procedure developed in [4], four first order differential equations are obtained and expressed in matrix form as

$$\begin{Bmatrix} u_B' \\ \varphi_z' \\ \varphi_y' \\ \rho' \end{Bmatrix} = [S]^{-1} \begin{Bmatrix} N_\xi \\ -M_\zeta \\ M_\eta \\ M_\omega \end{Bmatrix} - [S]^{-1} \cdot [S^*] \cdot \begin{Bmatrix} \psi' \\ \Omega' \\ \phi' \end{Bmatrix} \qquad (16)$$

[S] and [$S^*$] are rigidity matrices evaluated by the integration of the usual and the extended cross-section properties definitions. Hereby each element i of the cross-sectional area is multiplied by its own fictitious relationship $S_i$, and/or $G_i$

Eq.(16) and the following three definitions

$$\varphi_y = -w_B' , \varphi_z = v_B' \text{ and } \rho = \beta' \qquad (17)$$

give the stress resultant-displacement relationships.

## DETERMINATION OF THE ULTIMATE LOAD CAPACITY

The ultimate load capacity is defined as the load step at which the deformations continue to increase while the load ceases to do so. This condition occurs when either respectable zones along the beam are fully stressed to the plastic range i.e., equilibrium between the internal and external stress resultants is no longer satisfied, or the developed system of equations, due to the second order theory is unsolvable. When the shear deformation is included in the analysis the ultimate load capacity is also assumed to be reached when the equivalent strain of any cross sectional element equals a pre-defined maximum value representing the damaging strain of the used beam material.

The ultimate load capacity is determined within two nested calculation loops. The inner loop by which the rigidity matrices iteratively corrected until the internal and external stress resultants of each cross section are in equilibrium. The outer loop deals with the increase in the

proportional load until the ultimate load capacity is reached.

The developed computer program is based on the transport matrix method. The beam is divided into parts, Figure (5). Each part is divided into segments j to allow for the numerical integrations of the system of equations to determine the transport matrices. Finally each cross section k is discretized into elements, Figure (3). A summary of the inner loop is given hereafter.

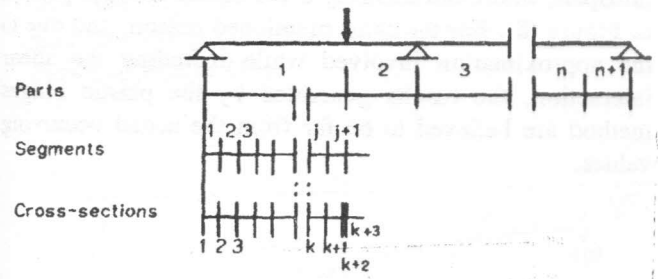


**Figure 5.** Beam's parts, segments, and cross sections.

For each cross section k the following mathematical operations are performed:

1- The external stress resultants are determined from the equilibrium equations, section 4.
2- For each cross section element i the normal and shear strains are calculated due to the linear terms of Eq.12 with the aid of the existing displacements. The equivalent strain $\in_e$ is then evaluated using Eq.11. The new corrected value of the secant modulues $S_i$ corresponding to the equivalent strain can be obtained according to the actual material relationship, Figure (4). Also the new values of the elastic plastic Poisson's ratio- and shear modulues are evaluated via Eq.6 and Eq.7 respectively. The new internal stresses can then be determined due to the new fictitious material relationships using Eqs.15.
3- When the previous step is completed for all elements of the cross section k, the rigidity matrices for this cross section $[S]_k$ and $[S^*]_k$ depending on the fictitious relationships and their inverts can be developed and prepared for the next iterative solution. Also, the internal stress resultants are calculated from the internal stresses according to their definitions. The integrations are carried out as summations of the forces developed from each cross sectional element.
4- A conversion is considered for the cross section k, when the relative difference between the internal and external stress resultants does not exceed a pre-defined small value.

## NUMERICAL EXAMPLES

The examples listed in this section are chosen to clearly illustrate the influence of including the effects of shear on various beam systems, and loading conditions. These examples have been treated previously in the literature, and have practical dimensions.

Example 1

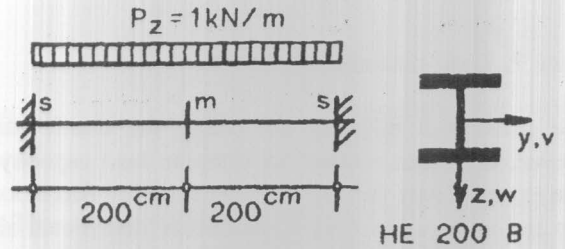


**Figure 6.** Example 1, Fixed ends beam loaded in the z-plane.

The linear system of the one-span beam with two fixed ends, Figure (6) is considered. It is loaded inplane at the center with a starting uniform load of 1 kN/m in the z-direction. The material relationship used is linear elastic-ideal plastic with a yield stress equals to 24 kN/cm$^2$ , elastic modulues E=21000 kN/cm$^2$ , and Poesson's ratio $\upsilon$=0.3. The equivalent strain is permitted up to 35 times the yield strain. These material coefficients are used for all the examples that follow. By increasing the load with a load factor $\alpha$ the ultimate load capacity is determined. To demonstrate the shear effects, the solution is obtained also by neglecting these effects. The load-deformation curve of the midspan vertical deflection plotted in Figure (7) shows an increase in the deformation by considering the shear effect within the elastic range by 27.3%. It is also showed that neglecting shear leads to an over estimation of the ultimate load capacity by 28.3%. Some comparisons are presented using other ultimate load theories.

Considering the interaction equations between bending moment M, normal force N and shearing force Q due to Windels [1], the ultimate load capacity is reached when the first two plastic hinges at the supports are formed due to the interaction between Q and M. They are calculated due to the linear elastic theory. At the ultimate load factor $\alpha_u$

$$(M_y)_{pl}=\alpha_u.p_z.L^2/12,(Q_z)_{pl}=\alpha_u.p_z.L/2$$

The load factor is found to be $\alpha_u = 107.6$

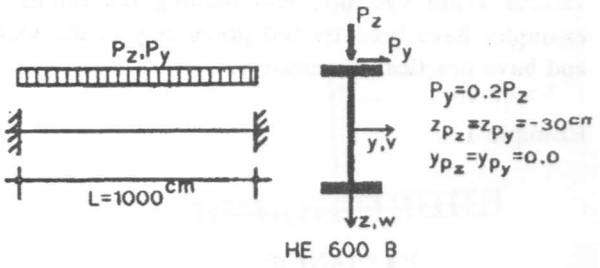


Figure 7. Load-deformation curve.

The stresses at midspan are within the elastic range, however, the beam reaches its ultimate load capacity.

The extreme case for fully plastic shearing force occurs when the web caries only a uniformly distributed shear stress with a maximum value of $\tau_{max}=\sigma_{yield}/\sqrt{3}$. The ultimate load factor is then equal to $\alpha_u=125.4$

Neglecting the shearing force, the failure occurs due to the plastic hinges theory when three plastic hinges are formed. In this case

$$2\,(M_y)_{pl} = \alpha_u \cdot p_z\, L^2/8$$

With a fully plastic bending moment results from the program, when neglecting shear effects, the ultimate load factor is found equals to $\alpha_u = 154.5$, using the above equation.

Table 1 shows the relative differences between the various theories

Table 1. Ultimate load factors for example 1.

| Method | $\alpha_u$ | Rel. Diff to last one |
|---|---|---|
| Plastic hinges neglecting shear | 154.5 | 28.75% |
| Plastic hinges with shear interaction due to [1] | 107.6 | -10.33% |
| Fully plastic shearing fore | 125.4 | 4.5% |
| Ref. [3] considering shear | 119.2 | -0.67% |
| Present analysis neglecting shear | 154 | 28.33% |
| Present analysis considering shear | 120 | 0% |

The result listed in table 1, due to the present theory considering shear effect agrees remarkably well with Ref [3]. Very close results are also found between the plastic hinges theory, and the present results when shear effects are neglected. The difference between the present exact study result and the plastic hinges method when shear interaction is included related to that the last method uses the elastic theory in calculating the stress resultants. By the exact method considering shear the bending moments at the supports begin to decrease due to shear interaction, starting for the load factor $\alpha = 110$. A comparison between the moments at the supports, and the moment at midspan, where the shearing force equals zero, is plotted in Figure (8). For the same mentioned reason, and due to the approximation involved while including the shear interaction, the results generated by the plastic hinges method are believed to be far from the actual occurring values.

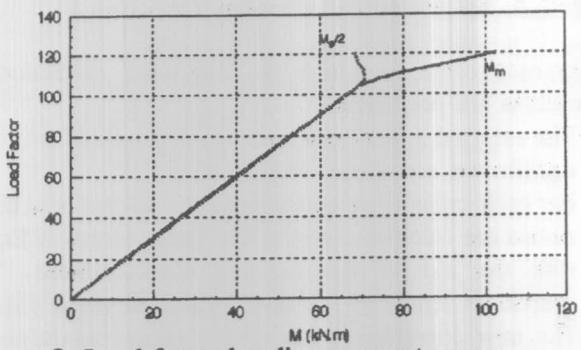


Figure 8. Load factor-bending moments curve

Example 2

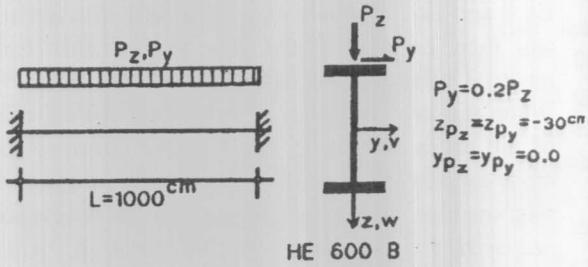


Figure 9. Example 2, Fixed ends beam spatially loaded

The totally fixed beam shown in Figure (9) is considered. It is spatially loaded with uniformly distributed vertical and horizontal loads acting at the middle of the upper flange. The system is chosen to demonstrate the effect of shear under torsional loadings on the ultimate load

shear under torsional loadings on the ultimate load capacity. A comparison is performed with a solution neglecting shear [6]. The load-centroid horizontal deformation curves are plotted in Figure (10). Both solutions are identical within the elastic range. However, taking the effect of shear into account leads to a reduction of about 3% in the ultimate load capacity. This reduction is due to the shear interaction by the warping torsion at the supports, and the high St. Venant torsion occurred near the supports. The distribution of these torsion moments along the span, at the ultimate load stage are shown in Figure (11).

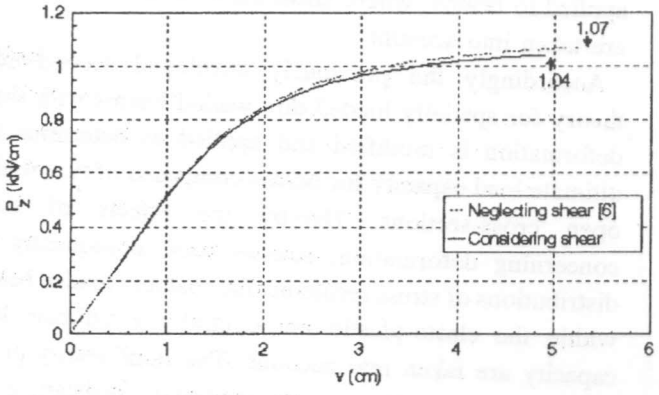


**Figure 10.** Load-Midspan horizontal deformation curve for example 2.

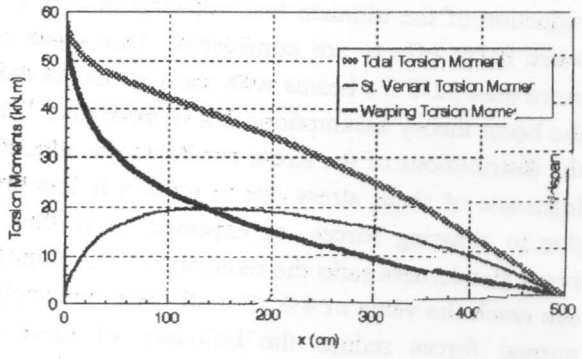


**Figure 11.** Distribution of torsion moments along the span at the ultimate load stage.

Example 3

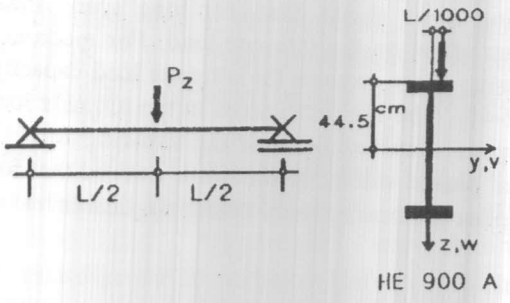


**Figure 12.** Example 3, Dimensions and system of loading.

The one span fork supported beam of Figure (12) is considered to investigate the effect of torsion and shearing force on the ultimate load capacity by variable beam spans. It is loaded with an eccentric concentrated single load applied at midspan in the vertical direction on the top chord. The eccentricity is always taken equal to one thousandth the span. The ultimate load capacities are obtained for several beam spans. The distributions of the ultimate moments $M_u$ relative to the full plastic moment $M_p$ with $L/L_y$ ratio are plotted in Figure (13). $L_y$ is defined in [3] as the beam span at which the torsional buckling stress has just reached the yield stress. $L_y$ value was given equals to 7.89 m in [3].

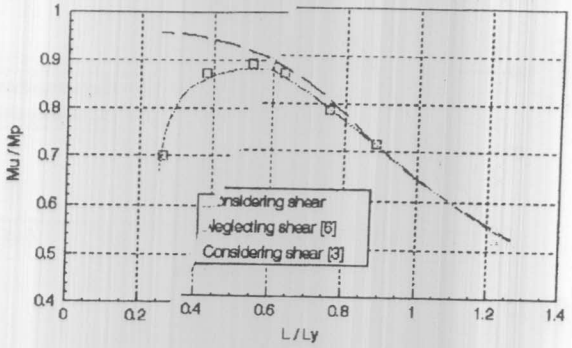


**Figure 13.** Ultimate load curves for fork supported one span beam due to eccentric single concentrated load.

Two ultimate load curves are plotted, as well, considering shear due to Maier [3] and neglecting shear due to Heil [6]. The present theory is well compared with Ref.[3]. The comparison with the ultimate load curve neglecting shear shows that, for long spans shear has minimum effect on the ultimate load. For medium spans considering shear reduces the ultimate load capacity with about 2-4%. The big differences in the ultimate loads for short spans occurred because the shearing forces reach their full plastic values. It should be noticed that for very short spans the beam theory is not applicable.

Example 4

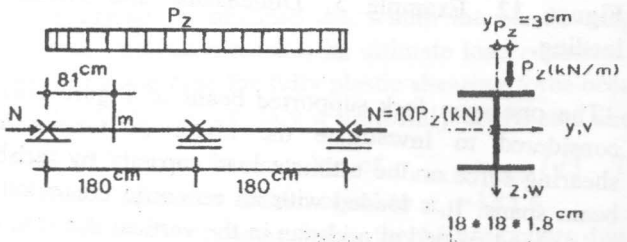


**Figure 14.** Example 4, Dimensions and loading

The spatially loaded continuous beam of Figure (14), previously treated elastically in [4], is considered. The loadings are increased to the ultimate load capacity of the system. The load-deflection curves, considering, as well as neglecting shear, are plotted in Figure (15).

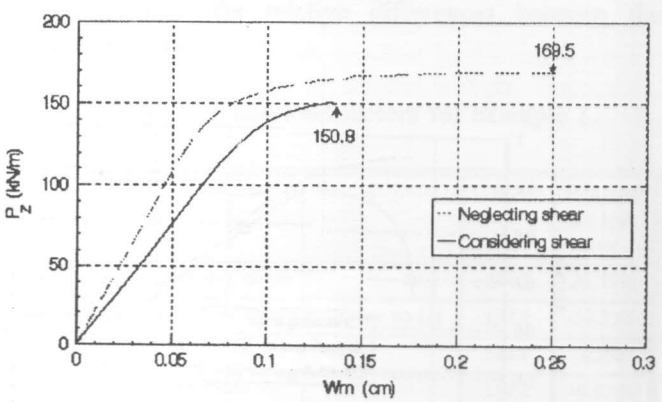


fig 15

**Figure 15.** Load-Deflection curve for example 4.

The linear inclinations of the curves within the elastic range agree with Ref.[4] where an increase in the deflections by 43% takes place when shear is considered. The ultimate load capacity is reduced in this case by about 11%. This value is small compared to the value obtained in example 1. The ultimate load capacities are evaluated for this example several times, using different more relative normal force loadings, which proves that shear effects decrease relatively with the application of the normal force. when the beam is no longer loaded by the normal force, the decrease of the ultimate load considering shear is found to be 32.5%.

## CONCLUSIONS

The general description of the constitutive behavior for isotropic materials is reduced to a finite constitutive law applied to beams, where shear stresses and deformations are taken into account.

Accordingly the previously developed second-order theory for spatially loaded thin walled beams with shear deformation is modified and applied to determine the ultimate load capacity for beams composed of thin walled open cross-sections. Hereby the effects of shear concerning deformation, stresses and subsequently the distributions of stress resultants for spatially loaded beams within the elasto-plastic range until the ultimate load capacity are taken into account. The nonlinearity of the equilibrium equations and material resistances is iteratively considered.

A comprehensive computer program is developed. Some practical systems are solved as examples. The comparison with other exact method considering all shear effects proves the accuracy of the developed technique.

It is also shown that the effect of shear should not be neglected. For practical dimensions and loadings a reduction of the ultimate load capacity of 28% is found when shear effects are considered. This value reaches more than 32% for beams with short spans but still obey the beam theory assumptions (l/h is more than 10). Also the distributions of the stress resultants are affected. The influence of shear stress due to torsion is less than that due to shearing forces, as expected. According to the beam slenderness ratio the reduction of the ultimate load can reach the value of 4%. For all cases, the applying of normal forces reduce the influence of shear on the ultimate load capacity. Finally the assumptions used to simplify the approximate methods dealing with shear effects can give unreliable solutions.

REFERENCES

[1] WINDELS, R.: Traglasten von Balkenquerschnitten bei Angriff von Biegemomente, Laengs-und Querkraft Der Stahlbau 1/1970.

[2] BAMM, D.: Naeherungsweise Berücksichtigung der Schubspannungen bei der Ermittlung von Traglasten gerader dünnwandiger Profile Disseertation TU Berlin 1974.

[3] MAIER, D.: Traglastberechnung raeumlicher Stabwerke aus Stahl und Leichtmetall unter Berücksichtigung der Schubweichheit Dissertation, Universitaet Karlsruhe, 1986.

[4] DIWAN, M.A.F.: Elastic Bending-Warping Second Order Theory For Continuous Beams Of Thin Walled Open Cross-Section With Shear Deformation Proc. Fourth Arab Structural Engineering Conference, Vol. I, PP. 301-314, Cairo, 1991.

[5] BETTEN, J.: Plastizitaetstheorie metallischer Werkstoffe Vorlesungsmitschrift Rhein.-Westf. Techn. Hochschule Aachen 1971.

[6] HEIL, W.: Traglastermittlung von raeumlich belasteten Durchlauftraegern mit offenem, dünwandigem Querscnitt bei beliebigem Werkstoffgesetz Dissertation Universitaet Karlsruhe 1979.